# Effect of following strength on pedestrian counter flow*

Kuang Hua(邝 华)[a)b)], Li Xing-Li(李兴莉)[c)], Wei Yan-Fang(韦艳芳)[a)d)], Song Tao(宋 涛)[a)], and Dai Shi-Qiang(戴世强)[a)†]

[a)] *Shanghai Institute of Applied Mathematics and Mechanics, Shanghai University, Shanghai* 200072, *China*
[b)] *College of Physics and Technology, Guangxi Normal University, Guilin* 541004, *China*
[c)] *School of Applied Science, Taiyuan University of Science and Technology, Taiyuan* 030024, *China*
[d)] *Department of Physics and Information Science, Yulin Normal University, Yulin* 537000, *China*

(Received 26 July 2009; revised manuscript received 16 November 2009)

This paper proposes a modified lattice gas model to simulate pedestrian counter flow by considering the effect of following strength which can lead to appropriate responses to some complicated situations. Periodic and open boundary conditions are adopted respectively. The simulation results show that the presented model can reproduce some essential features of pedestrian counter flows, e.g., the lane formation and segregation effect. The fundamental diagrams show that the complete jamming density is independent of the system size only when the width $W$ and the length $L$ are larger than some critical values respectively, and the larger asymmetrical conditions can better avoid the occurrence of deadlock phenomena. For the mixed pedestrian flow, it can be found that the jamming cluster is mainly caused by those walkers breaking the traffic rules, and the underlying mechanism is analysed. Furthermore, the comparison of simulation results and the experimental data is performed, it is shown that this modified model is reasonable and more realistic to simulate and analyse pedestrian counter flow.

**Keywords:** following behaviour, lattice gas model, counter flow
**PACC:** 0550, 0520

## 1. Introduction

In recent years, pedestrian flow has attracted considerable attention in the field of physical science and engineering.[1−3] The complex behaviours of pedestrian can result in many interesting self-organisation phenomena and collective behaviours, e.g., jamming and clogging, lane formation and oscillations at bottlenecks in counter flow, freezing by heating, faster-is-slow effect and herding behaviour in panic situations, and all those have been successfully reproduced with physical methods.[4−7] Therefore, to gain an insight into complex behaviours of pedestrians and predict them are particularly valuable in many different areas of application such as an optimisation of pedestrian facilities, urban and traffic planning, building evacuation, etc.

The modeling of pedestrian behaviours can be classified into two main categories: macroscopic and microscopic models. The former describes pedestrians with fluid-like properties, and the different individuals can not be distinguished, e.g., the hydrodynamic models.[8,9] In contrast, the latter describes the spatiotemporal behaviours of individual pedestrians, and the different types of pedestrians with individual properties, such as the social force models,[10,11] cellular automata models,[12−20] lattice gas models[21−33] and agent-based models.[34] Since microscopic models can better characterise the different behaviours of pedestrian, they have been extensively applied to simulate the emergency evacuation,[19−21] counter channel flow,[22−31] and bottleneck flow.[32] Especially, in the last years the lattice gas model are successful in investigating such many pedestrian behaviours in counter flow as right-moving preference behaviour,[16] the traffic rule breaking behaviour,[25] exchanging positions and back step behaviours,[26,27] mobile robot's behaviour,[28] sidling and turning movement behaviours,[29,33] and mixed walking behaviours of different velocities,[30] etc.

Recently, the authors have found that subconscious behaviours play an important role in enhancing the critical current and density in counter flow.[22,23] In our research, subconscious behaviours are manifested in the following three aspects. First, walkers are accustomed to walking along the right-hand side of the road considering the traffic rules and customs. Secondly, when the opposite direction walkers encounter

*Project supported by the National Basic Research Program of China (Grant No. 2006CB705500), and the National Natural Science Foundation of China (Grant Nos. 10962002, 10902076 and 10532060).
†Corresponding author. E-mail: sqdai@shu.edu.cn
© 2010 Chinese Physical Society and IOP Publishing Ltd

each other, they prefer to move respectively from their right-hand side in order to avoid collision. Finally, fast walkers are used to overtaking the preceding walkers in the same direction from the left-hand side of the road. However, the following behaviour of pedestrians during walking, i.e., waiting probability has not been considered. In addition, some researchers have studied the following effect,[15,26] but the strength of following behaviour has not been perfectly distinguished from the different scenarios. That is to say, waiting probability is always regarded as a constant for all situations in the numerical simulation. Therefore, further studies on the following behaviour are still necessary to understand the underlying mechanism of pedestrian dynamics. In general, when pedestrians walk, they would decide whether to accelerate and change direction or not according to local environment. Obviously, the different local environment could give rise to different following behaviours, and the waiting probability would change correspondingly. For example, when the preceding pedestrian walks at the same speed and direction with the current one, he/she will not usually change moving direction and prefer to follow the movement, and thus the strength of following behaviour (i.e., the waiting probability) is relatively large. Whereas, when the preceding pedestrian moves at the low speed in the same direction, he/she is accustomed to exceeding from his/her left-hand side, and correspondingly the strength of following behaviour is small. How do these scenarios affect the pedestrian dynamics in the counter flow? This is an interesting but still open problem.

In this paper, our primary aim is to integrate subconscious behaviours[23] with the action-selection mechanism where each walker makes a judgment of the preferential moving direction (i.e., left, right, forward and wait behind) according to its perception of the different situations, and hope to better reflect realistic pedestrian behaviours. We present a modified lattice gas model to investigate the pedestrian counter flow by considering the different strengths of following behaviour and the various behaviour habits under the periodic and open boundary conditions. The pedestrian dynamics and the underlying mechanism of jam are discussed in greater detail.

## 2. Model

The model is defined on a square lattice of $W \times L$ sites, where $W$ and $L$ are respectively the width and length of the channel. There are four classes of pedestrians with no back step in this system: the faster or slower right walkers going from the left to the right and the faster or slower left walkers going from the right to the left. The size of a site corresponds to approximately 0.4 m $\times$ 0.4 m. This is the typical space occupied by a person in a dense crowd.[12] Fast walkers can move quickly forward two grids per time-step, and slow walkers can move one grid per time-step. Empirically, the average velocity of a pedestrian is about 1.6 m/s for a faster walker or 0.8 m/s for a slower walker under normal conditions,[35] so one time-step is approximately 0.5 s in our model. When the walker arrives at the wall of the channel, it is reflected by the wall and never goes out through the wall. The two types of boundaries are used herein.

Figures 1 and 2 respectively give the possible configurations of the slower and faster right walkers going to the right. The full circle indicates the right walker with velocity $V_1$. The cross point indicates the site occupied by another walker with velocity $V_2$, and corresponding moving direction is denoted by slender arrows. Each walker can only move to the unoccupied sites or stand. The bold arrow indicates the possible moving directions (the right, up, down and still) of the right walker, and the corresponding transition probabilities are given by $P_{t,x}$, $P_{t,y}$, $P_{t,-y}$ and $P_w$ respectively.

In order to reflect realistic pedestrian behaviours, the transition probabilities are established by the following rules.

For a slower right walker, (1) if the front cell is occupied by a same direction walker (slower or faster right walker), the waiting probability $P_w$ is higher. The reason is that walkers generally prefer to persist in their present direction and follow others in the same direction, e.g., in Figs. 1(c) and 1(f); (2) if the front cell is occupied by an opposite walker, the probability $P_{t,-y}$ of right direction is higher, because walkers have the priority to move on their right-hand sides in order to avoid collision and keep safety, e.g., in Figs. 1(b) and 1(e). Especially, in Fig. 1(d), when the front and right cells are occupied, the waiting probability $P_w$ is also higher. That is because if the preceding walker is a left walker, the walker usually would rather stop than move to the left cell so as to obey right-walking traffic rule. In addition, if the preceding walker is a right walker, the following behaviour will appear due to the above mentioned reason.

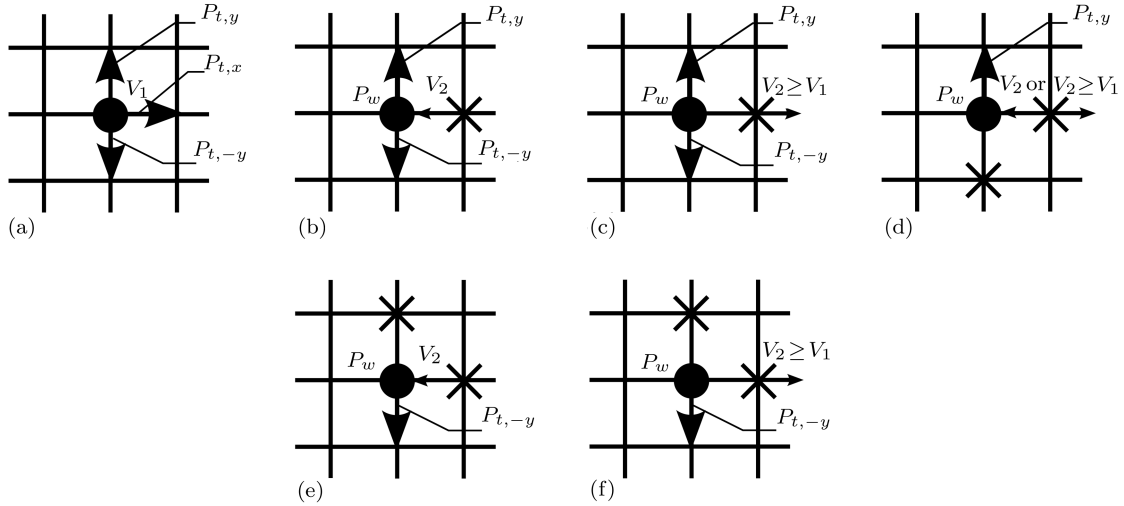



**Fig. 1.** The possible configurations of the slower right walkers.

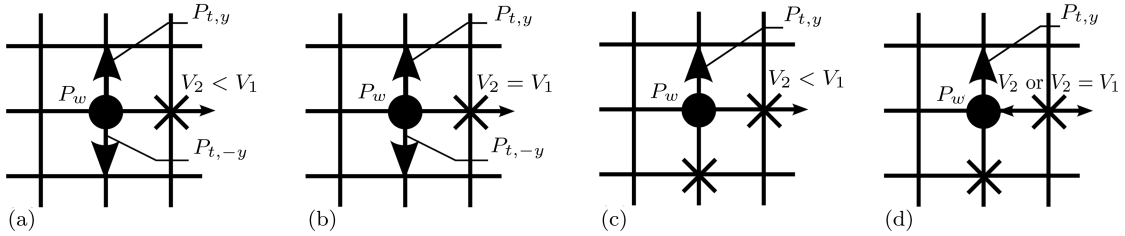



**Fig. 2.** The possible configurations of the faster right walkers.

For a faster right walker, (1) if the front cell is occupied by a slower right walker, the probability $P_{t,y}$ of left direction is higher, because the faster walkers would be accustomed to overtaking the preceding slower walkers in the same direction from the left-hand side, e.g., in Figs. 2(a) and 2(c); (2) if the front cell is occupied by a faster right walker or a left walker, the waiting probability $P_w$ is higher due to following effect and right-walking traffic rule, e.g., in Figs. 2(b) and 2(d).

Based on the above analysis, the transition probabilities $P_{t,x}$, $P_{t,y}$, $P_{t,-y}$ of the right walker corresponding to each configuration are given as follows:

$P_{t,x} = D_1 + (1 - D_1)/3$, $P_{t,y} = (1 - D_2)(1 - D_1)/3$, $P_{t,-y} = (1 + D_2)(1 - D_1)/3$ and $P_w = 0$ for Fig. 1(a);
$P_{t,x} = 0$, $P_{t,y} = (1 + D_2)(1 - D_1)/3$, $P_{t,-y} = D_1 + (1 - D_1)/3$ and $P_w = (1 - D_2)(1 - D_1)/3$ for Fig. 1(b);
$P_{t,x} = 0$, $P_{t,y} = (1 - D_2)(1 - D_1)/3$, $P_{t,-y} = (1 + D_2)(1 - D_1)/3$ and $P_w = D_1 + (1 - D_1)/3$ for Fig. 1(c);
$P_{t,x} = 0$, $P_{t,y} = (1 + D_2)(1 - D_1)/2$, $P_{t,-y} = 0$ and $P_w = D_1 + (1 - D_2)(1 - D_1)/2$ for Fig. 1(d);
$P_{t,x} = 0$, $P_{t,y} = 0$, $P_{t,-y} = D_1 + (1 - D_2)(1 - D_1)/2$ and $P_w = (1 + D_2)(1 - D_1)/2$ for Fig. 1(e);
$P_{t,x} = 0$, $P_{t,y} = 0$, $P_{t,-y} = (1 + D_2)(1 - D_1)/2$ and $P_w = D_1 + (1 - D_2)(1 - D_1)/2$ for Fig. 1(f);
$P_{t,x} = 0$, $P_{t,y} = D_1 + (1 - D_1)/3$, $P_{t,-y} = (1 - D_2)(1 - D_1)/3$ and $P_w = (1 + D_2)(1 - D_1)/3$ for Fig. 2(a);
$P_{t,x} = 0$, $P_{t,y} = (1 + D_2)(1 - D_1)/3$, $P_{t,-y} = (1 - D_2)(1 - D_1)/3$ and $P_w = D_1 + (1 - D_1)/3$ for Fig. 2(b);
$P_{t,x} = 0$, $P_{t,y} = D_1 + (1 + D_2)(1 - D_1)/2$, $P_{t,-y} = 0$ and $P_w = (1 - D_2)(1 - D_1)/2$ for Fig. 2(c);
$P_{t,x} = 0$, $P_{t,y} = (1 - D_2)(1 - D_1)/2$, $P_{t,-y} = 0$ and $P_w = D_1 + (1 + D_2)(1 - D_1)/2$ for Fig. 2(d);

where $D_1$ indicates the strength of the drift pointing to the exits (right or left), and $D_2$ represents the strength of the preferential direction of subconscious behaviour. Also, the transition probabilities of a right walker are obtained for other configurations.[23] For a left walker, similar prescriptions can be given for the possible configurations in the same way.

## 3. Simulation results and discussions

We carry out the simulation for the above model under the periodic boundary condition. Initially, the pedestrians of four types are distributed randomly within the channel, and the random sequential update is used. In this paper, we introduce two new parameters $m$ (the ratio of the number of the right walkers to the number of all walkers) and $f$ (the ratio of the number of the fast walkers to the number of all walkers). In the simulations, the related parameters are selected as $W = 20$, $L = 100$, $D_1 = 0.6$, $D_2 = 0.9$, $m = 0.5$, $f = 0.5$ unless otherwise mentioned.

The mean velocity in one update time step is defined as the sum of the velocities of walkers moving forward divided by the total number of walkers existing in the system. The mean flow is defined as the sum of the number of the right walkers moving through the right boundary and that of the left ones moving through the left boundary in one update time step. For each simulation, 10000 time steps are carried out, and the value of the mean velocity and mean flow are computed according to the last 4000 time steps averaged over 20 different random initial pedestrian distributions, although in all our simulations it takes no more than 2000 time steps to reach the steady states.

First, we investigate the effect of system size on the mean velocity and the mean flow. Figure 3 shows the fundamental diagram for different system sizes $W \times L = 10 \times 100$, $20 \times 100$, $40 \times 100$, $60 \times 100$, $80 \times 100$ for (a), and $W \times L = 20 \times 20$, $20 \times 60$, $20 \times 100$, $20 \times 200$, $20 \times 300$ for (b), respectively. From Fig. 3(a), it can be clearly seen that in the freely moving phase, the mean velocity decreases with the increase of $W$, however, the mean flow is proportional to width $W$. This is because at the same density, the number of total walkers becomes larger with the increase of $W$, which hints that the nonlinear interaction among walkers will be strengthened, and leads to the decrease of mean velocity correspondingly. Meanwhile, a larger $W$ is contributive to the increase of mean flow according to the calculation of its definition above mentioned. In addition, we find that the completely jamming density increases with the increase of $W$, nevertheless, When $W \geq 40$, it has almost an unvarying value $\rho_{\rm jam} = 0.72$, which indicates that the completely jamming density does not depend on the system sizes when $W$ is larger than a certain value.

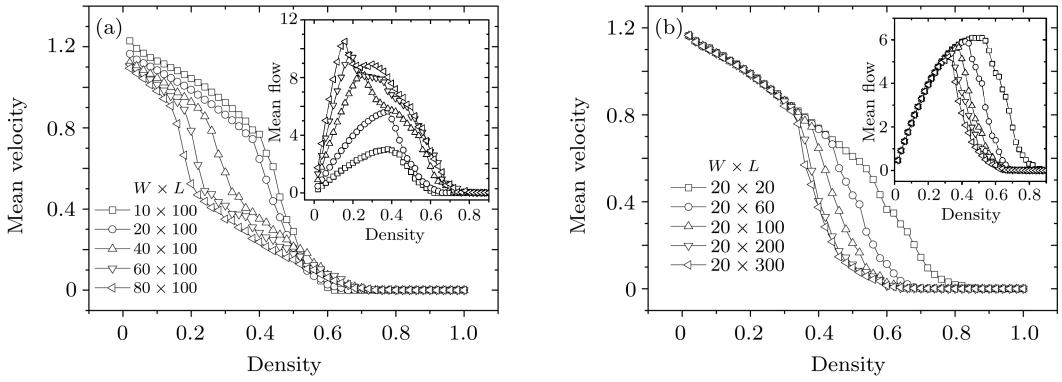



**Fig. 3.** Plot of the mean velocity and the mean flow against the density with different system sizes.

Figure 3(b) shows that the mean velocity (flow) linearly decreases (increases) with increasing density and completely equals each other for the values of different length $L$ at the beginning, after that, it declines quickly to zero. We find that the complete jamming density decreases with the increase of $L$. However, when $L \geq 100$, it almost remains a constant value $\rho_{\rm jam} = 0.64$, which indicates that the jamming transition point is independent of the system sizes when $L$ is larger than a certain value.

Comparing Fig. 3(a) with Fig. 3(b), we find that at the same area, e.g., $W \times L = 60 \times 100$ in Fig. 3(a) and $W \times L = 20 \times 300$ in Fig. 3(b), the larger width $W$ shows the better ability to improve the mean flow and the completely jamming density than the larger length $L$. Therefore, a useful conclusion is drawn that increasing width $W$ may be more beneficial than increasing length $L$ under the same area during planning

building design when we consider the emergency evacuation.

In order to gain a deep insight into the effect of the asymmetric system, we study the variation of the mean velocity and the mean flow under the asymmetrical conditions for the different number of left and right walkers in the system. Figure 4 gives the three dimensional (3D) plot of the mean velocity (a) and the mean flow (b) against the density and parameter $m$. We find that the values of mean velocity and the mean flow are not completely symmetric for $m > 0.5$ (i.e., the number of the right walkers is larger than that of the left walkers) and $m < 0.5$ (i.e., the number of the left walkers is larger than that of the right walkers) because of the existence of statistical error and the influence of random distribution during the calculation and simulation. It should be noted that for larger asymmetrical bidirectional flows such as $m \in [0, 0.25]$ and $m \in [0.75, 1]$, the completely jamming densities are relatively larger than those of $m \in (0.25, 0.75)$, where the counter flow is nearly separated to two independent opposite unidirectional flows, and the interaction among opposite walkers will be weakened, therefore, the jams will obviously decrease, and deadlock phenomena (i.e., bidirectional pedestrian flow will easily form completely jamming phase at low density for cellular automata model and lattice gas model in the simulation, it is an unrealistic situation for real life)[36] at higher density will also be better avoided. All these reflect that reasonable control and application of asymmetric information have a positive effect at higher density for the improvement of road utilisation.

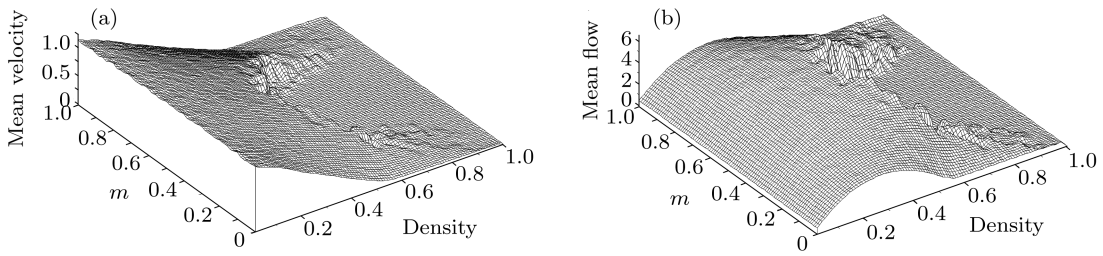



**Fig. 4.** The 3D plots of the mean velocity (a) and the mean flow (b) against density and $m$.

Now, we will focus on analysing the influence of the faster walkers in the system. Figure 5 gives the plot of the mean velocity and the mean flow against density. One can see that at the free moving phase, the mean velocity and the mean flow increase with the increase of $f$. However, the complete jamming transition point is approximately equal for $f > 0$, and its value is smaller than that of $f = 0$. The reason is that at the low density, the walkers have enough space to move in the channel, in such case, the increase of faster walkers can lead to the increase of both the mean velocity and the mean flow. Nevertheless, at the large density, the total number of pedestrians becomes larger and the interaction of walkers becomes stronger due to the decrease of available space. Especially with the further increase of the number of faster walkers, they will walk in the left-hand side of channel in order to overtake the front slower walkers from their left-hand side, occupy the lane of opposite walkers and hamper the free movement of the opposite walkers. As a result, with the strengthening of their interaction, mini-jams occur and finally form the completely mega-jams. Based on the above analysis, we can conclude that the overtaking movement of faster walker may be one of the main factors for inducing jamming at the large density.

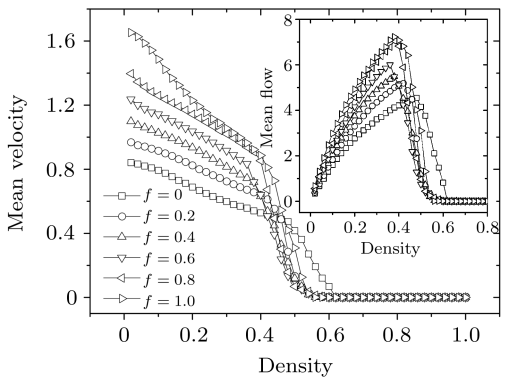



**Fig. 5.** Plot of the mean velocity and the mean flow against density at $f = 0, 0.2, 0.4, 0.6, 0.8, 1.0$.

What would happen if some pedestrians break the traffic rules (i.e., $D_2 = 0$, all pedestrians can not

walk according to subconscious behaviour rules) in the counter flow? This is a significant problem for mixed pedestrian flow. We introduce a dimensionless coefficient $R$, denoting the ratio of the number of pedestrian breaking the traffic rules to the number of all pedestrians. Figure 6 shows the plot of the mean velocity and the mean flow against density at $R = 0.0, 0.1, 0.3, 0.5, 0.7, 1.0$. We can clearly see when the density is low, the mean velocity (the mean flow) decreases (increases) linearly with the increase of the density. When the density further increases, the mean velocity and the mean flow abruptly decrease and become zeros, in such a case, the consciousness of obeying or breaking the traffic rules have no obvious influence on the mean velocity and flow except for the critical density which decreases gradually with the increase of $R$. Here, it should be noted when $R = 0$ (i.e., all pedestrians obey the traffic rules in the system), the maximum values of the critical density and the mean flow are much larger in comparison with those of $R > 0$ (i.e., some pedestrians break the traffic rules in the system).

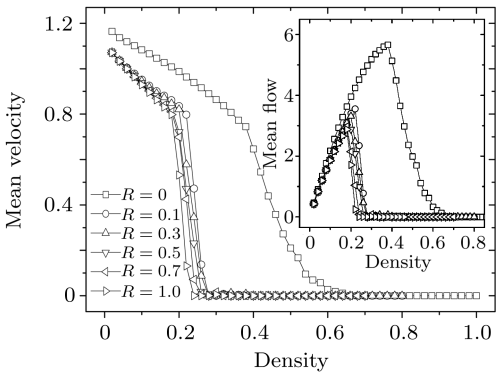



**Fig. 6.** Plot of the mean velocity and the mean flow against density at $R = 0, 0.1, 0.3, 0.5, 0.7, 1.0$.

We explore the related intrinsic mechanism of Fig. 6. To a large extent, the walkers breaking the traffic rules can strongly disturb others' behaviour habits and judgments about the preferential moving direction. As a result, some blind followers also break the traffic rules. With the time evolution, this turbulence will be rapidly expanded, at the same time, the nonlinear interactions among walkers will be strengthened quickly and the phase transition happens eventually. All these reflect that the walkers breaking the traffic rules have an important influence on the pedestrian counter flow, and mistaken navigation and blind following are the underlying mechanism for inducing the jams. A useful suggestion can be proposed for pedestrian evacuation that the correct navigation information (e.g., the indicative mark) at the emergence exits is necessary to avoid blind following and improve evacuation efficiency.

Next we investigate the patterns of pedestrian counter flow. Figure 7 gives the typical patterns obtained at $\rho = 0.3$, where eight types of pedestrian are indicated, respectively, by open right triangle (circles) and open left triangles (pentacles) for the faster (slower) right and left walkers obeying the traffic rules, and full right triangles (circles) and full left triangles (pentacles) for the faster (slower) right and left walkers breaking the traffic rules. The pattern (a) shows the freely moving phase obtained at $R = 0$. We can see clearly that there are six evident separate lanes which are composed of the different types of walkers in the channel. From top to bottom, the first lane is fully occupied by the slower left walkers, the second by the faster and slower left walkers, the third almost by the faster left walkers near the central partition line, the fourth mainly by the faster right walkers, the fifth by the faster and slower right walkers and the sixth by the slower right walkers. In addition, an interesting feature is found that the second and the fifth lanes are broad-sparse for mixed walkers in comparison with those of other lanes for pure walkers. This segregation effect of lane formation is the result of the pedestrian action-selection and decision-making. This phenomenon is also in agreement with the experiential result in real life. The patterns (b)–(d) show the time evolution of the jamming transition for $R = 0.1$ at $t = 300, 420, 600$, respectively. In the beginning, most pedestrians can move freely. At the same time, small jam clusters form (see Fig. 7(b)), and finally become a complete blockage with time evolution (see Fig. 7(d)). All these results are consistent with the above analysis. In addition, we also gain a deep understanding that obeying the traffic rules could effectively decreases the occurrence of jam cluster.

We also study the effect of the strength of subconscious behaviour on jamming transition. Figure 8 shows the plot of the mean velocity and the mean flow against density at $D_2 = 0, 0.3, 0.6, 0.9, 1.0$ and $R = 0$. When $D_2 < 1$, we can clearly see that with increase of $D_2$, the jam transition threshold, the mean velocity and the mean flow increase. However, when $D_2 = 1$, a surprising phenomenon is discovered that the values of mean velocity and the mean flow are not maximal at $\rho \in [0.18, 0.42]$. This is because all pedestrians can only mechanically move according to behaviour rules,

similar to the movement of robot for $D_2 = 1$. At the middle density, this kind of mechanical moving not only can strengthen the interaction among pedestrians and form small jam clusters, but also can break up the small clusters more easily when the jammed pedestrians in these clusters succeed in moving pass each other (i.e., the clusters are dissolved) according to these definitive behaviour rules. In such a case, with the time evolution, the mean velocity tends to be a stable value and the system runs into a metastable state. In addition, the critical density is the highest for $D_2 = 1$, which means that although mechanical moving neglects the complexity and randomicity of pedestrian movement, it has a positive effect for decreasing the occurrence of jam cluster.

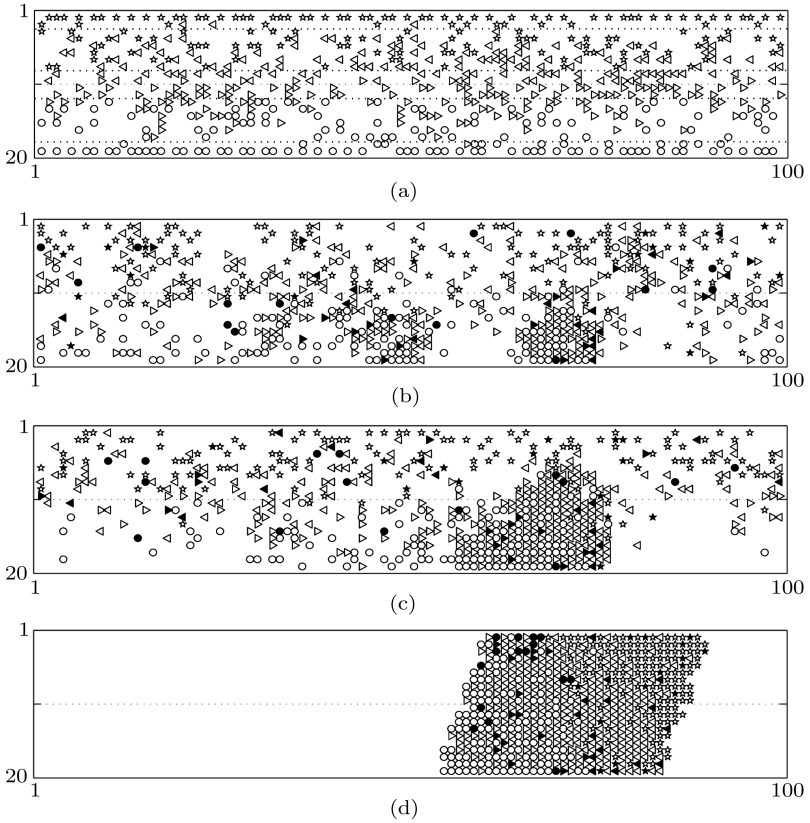



**Fig. 7.** The typical patterns obtained at $\rho = 0.3$. The pattern (a) shows the freely moving phase obtained at $R = 0$, $t = 1000$. The patterns (b)–(d) show the time evolution of the completely jamming transition at $R = 0.1$; (b) the pattern obtained at $t = 300$; (c) the pattern obtained at $t = 420$; (d) the pattern obtained at $t = 600$.

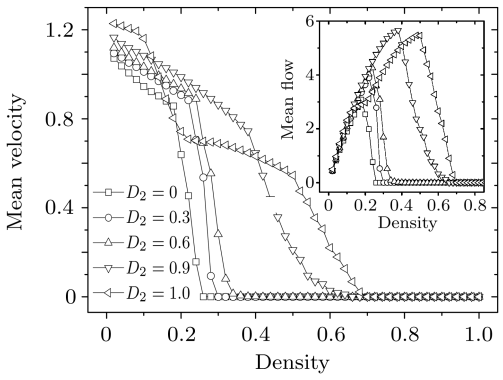



**Fig. 8.** Plot of the mean velocity and the mean flow against density at $D_2 = 0, 0.3, 0.6, 0.9, 1.0$, and $R = 0$.

Finally we implement a comparison between our model and the experimental result which was given by Isobo *et al.*[31] In the experiments, $L = 30$, $W = 5$ the left and right boundaries are open and left and right walkers are randomly distributed in the right and left half of the channel, respectively. Figure 9 presents the comparison of the simulation and the experiment, where the model in this paper is called model 1, and the model of subconscious behaviour is referred to as model 2.[23]

Figure 9(a) shows the plot of the mean arrival time against density. We find that model 1 is almost in agreement with experiment at $\rho < 0.34$, however

with the further increase of density, simulation results deviate from experiment quickly. The reason is that some jams are observed in simulations due to the effect of random initial distribution and no back step for pedestrians, but no jams in experiments. It reflects a fact that the human intelligence and flexibility are too complex to be presented perfectly with simple models.

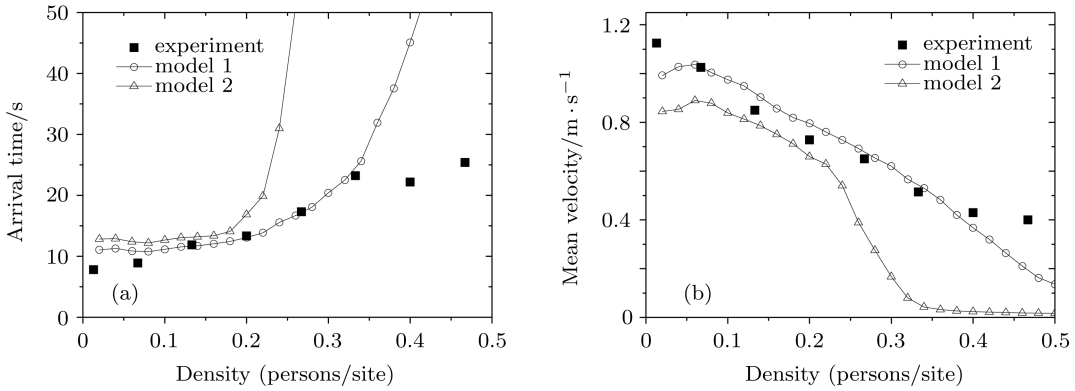



**Fig. 9.** The comparison of the simulation and experiment.

Figure 9(b) shows the plot of the mean velocity against density. For model 1, when $\rho \in [0.06, 0.36]$, the mean velocity is a little higher, because the faster walkers is considered in model. For model 2, the mean velocity is always smallest, and when $\rho > 0.22$, the mean velocity decreases quickly to zero, however, the mean velocity decreases slowly and can not be equal to zero for model 1. It indicates that model 1 can effectively decrease the occurrence of jam and alleviate deadlock problem. The comparative results show that the modified model can better describe real pedestrian counter flow.

## 4. Summary and outlook

Our aim in this paper is to deliver a better exploration of the effect of following strength on pedestrian counter flow. To do so, we have proposed a modified lattice gas model, in which the waiting probabilities under different situations are elaborated. Through numerical simulations and comparison with the empirical data, it can be concluded that: (i) the presented model can reproduce some essential features of pedestrian counter flows, such as the lane formation and segregation effect; (ii) the complete jamming density does not depend on the system size only when the width $W$ and the length $L$ are larger than some critical values respectively; (iii) the larger asymmetrical condition can obviously avoid deadlock problem; (iv) the walkers obeying the traffic rules can effectively decrease the occurrence of jam; (v) the mean velocity (flow) and the jam transition threshold increase with increasing $D_2$; (vi) the presented model shows the better superiority in describing real pedestrian counter flow.

In summary, the primary results here can be useful for emergency evacuation planning and pedestrian facilities design, e.g., to make an indicative mark at the emergency exit to avoid blind following behaviours, separate right and left walkers by a partition line in the channel to prevent collision among opposite pedestrians, etc. In our future work, the presented model will be extended to investigate more general situations such as pedestrian overbridge, pedestrian crosswalk, etc.

## References

[1] Waldau N, Gattermann P, Knoflacher H and Schreckenberg M 2007 *Pedestrian and Evacuation Dynamic 2005* (Berlin: Springer-Verlag)

[2] Nagatani T 2002 *Rep. Prog. Phys.* **65** 1331

[3] Robin T, Antonini G, Bierlaire M and Cruz J 2009 *Trans. Res.* B **43** 36

[4] Helbing D, Farkas I J and Vicsek T 2000 *Phys. Rev. Lett.* **84** 1240

[5] Helbing D, Farkas I J and Vicsek T 2000 *Nature* **407** 487
[6] Muramatsu M, Irie T and Nagatani T 1999 *Physica* A **267** 487
[7] Muramatsu M and Nagatani T 2000 *Physica* A **286** 377
[8] Hughes R L 2003 *Ann. Rev. Fluid Mech.* **35** 169
[9] Xia Y H, Wong S C and Shu C W 2009 *Phys. Rev.* E **79** 066113
[10] Helbing D and Molnar P 1995 *Phys. Rev.* E **51** 4282
[11] Helbing D, Buzna L, Johansson A and Werner T 2005 *Trans. Sci.* **39** 1
[12] Burstedde C, Klauck K, Schadschneider A and Zittartz J 2001 *Physica* A **295** 507
[13] Blue V J and Adler J L 2001 *Trans. Res.* B **35** 293
[14] Yu Y F and Song W G 2007 *Phys. Rev.* E **75** 046112
[15] Weng W G, Chen T, Yuan H Y and Fan W C 2006 *Phys. Rev.* E **74** 036102
[16] Yang L Z, Li J and Liu S B 2008 *Physica* A **387** 3281
[17] Yue H, Shao C F, Chen X M and Hao H R 2008 *Acta Phys. Sin.* **57** 6901 (in Chinese)
[18] Zhou J W, Chen X L, Zhou J H, Tan H L, Kong L J and Liu M R 2009 *Acta Phys. Sin.* **58** 2281 (in Chinese)
[19] Huang H J and Guo R Y 2008 *Phys. Rev.* E **78** 021131
[20] Liu S B, Yang L Z, Fang T Y and Li J 2009 *Physica* A **388** 1921
[21] Helbing D, Isobe M, Nagatani T and Takimoto K 2003 *Phys. Rev.* E **67** 067101
[22] Kuang H, Song T, Li X L and Dai S Q 2008 *Chin. Phys. Lett.* **25** 1495
[23] Kuang H, Li X L, Song T and Dai S Q 2008 *Phys. Rev.* E **78** 066117
[24] Takimoto K, Tajima Y and Nagatani T 2002 *Physica* A **308** 460
[25] Yu Y F and Song W G 2007 *Phys. Rev.* E **76** 026102
[26] Li J, Yang L H and Zhao D L 2005 *Physica* A **354** 619
[27] Ito S, Nagatani T and Saegusa T 2007 *Physica* A **373** 672
[28] Weng W G, Shen S F, Yuan H Y and Fan W C 2007 *Physica* A **375** 668
[29] Fukamachi M and Nagatani T 2007 *Physica* A **377** 269
[30] Jiang R and Wu Q S 2007 *Physica* A **373** 683
[31] Isobe M, Adachi T and Nagatani T 2004 *Physica* A **336** 638
[32] Tajima Y, Takimoto K and Nagatani T 2001 *Physica* A **294** 257
[33] Matsui A, Mashiko T and Nagatani T 2009 *Physica* A **388** 157
[34] Perez G J and Saloma C 2009 *Physica* A **388** 2469
[35] Schadschneider A, Klingsch W, Klüpfel H, Kretz T, Rogsch C and Seyfried A 2009 *Encyclopedia of Complexity and System Science* (Vol. 3) (Berlin: Springer) p3142
[36] Kretz T, Kaufman M and Schreckenberg M 2008 *Cellular Automata-8th International Conference on Cellular Automata for Research and Industry* (Berlin: Springer) p555